Taylor & Francis Group

Acta Oncologica

First system for fully-automated multi-criterial treatment planning for a high-magnetic field MR-Linac applied to rectal cancer

Rik Bijman, Linda Rossi, Tomas Janssen, Peter de Ruiter, Casper Carbaat, Baukelien van Triest, Sebastiaan Breedveld, Jan-Jakob Sonke & Ben Heijmen

Published online: 21 May 2020.

Submit your article to this journal ↗

Article views: 413

View related articles ↗

View Crossmark data ↗

Taylor & Francis
Taylor & Francis Group

ORIGINAL ARTICLE

First system for fully-automated multi-criterial treatment planning for a high-magnetic field MR-Linac applied to rectal cancer

Rik Bijman[a] , Linda Rossi[a], Tomas Janssen[b], Peter de Ruiter[b], Casper Carbaat[b], Baukelien van Triest[b], Sebastiaan Breedveld[a], Jan-Jakob Sonke[b] and Ben Heijmen[a]

[a]Department of Radiation Oncology, Erasmus MC Cancer Institute, Rotterdam, The Netherlands; [b]Department of Radiation Oncology, The Netherlands Cancer Institute, Amsterdam, The Netherlands

ABSTRACT

Background and purpose: In this study we developed a workflow for fully-automated generation of deliverable IMRT plans for a 1.5 T MR-Linac (MRL) based on contoured CT scans, and we evaluated automated MRL planning for rectal cancer.

Methods: The Monte Carlo dose calculation engine used in the clinical MRL TPS (Monaco, Elekta AB, Stockholm, Sweden), suited for high accuracy dose calculations in a 1.5 T magnetic field, was coupled to our in-house developed Erasmus-iCycle optimizer. Clinically deliverable plans for 23 rectal cancer patients were automatically generated in a two-step process, i.e., multi-criterial fluence map optimization with Erasmus-iCycle followed by a conversion into a deliverable IMRT plan in the clinical TPS. Automatically generated plans (AUTOplans) were compared to plans that were manually generated with the clinical TPS (MANplans).

Results: With AUTOplanning large reductions in planning time and workload were obtained; 4–6 h mainly hands-on planning for MANplans vs $\sim$1 h of mainly computer computation time for AUTOplans. For equal target coverage, the bladder and bowel bag D_{mean} was reduced in the AUTOplans by 1.3 Gy (6.9%) on average with a maximum reduction of 4.5 Gy (23.8%). Dosimetric measurements at the MRL demonstrated clinically acceptable delivery accuracy for the AUTOplans.

Conclusions: A system for fully automated multi-criterial planning for a 1.5 T MR-Linac was developed and tested for rectal cancer patients. Automated planning resulted in major reductions in planning workload and time, while plan quality improved. Negative impact of the high magnetic field on the dose distributions could be avoided.
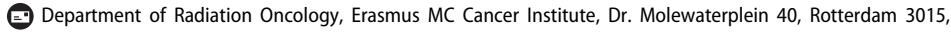
Introduction

With the introduction of MR-Linac (MRL) treatment units [1,2], the demand for high quality treatment plans has further increased to guarantee maximum benefit of the advanced but expensive in-room MR-guidance. Treatment sites in the pelvic area, including rectal tumors, are known to be affected by large motions and anatomy variations [3] and are therefore interesting candidates for MRL treatment [4].

The unique characteristics and design of the Unity MRL (Elekta AB, Stockholm, Sweden), investigated in this study, brings up treatment planning challenges compared to conventional linac treatment. Only a 7 MV FFF beam is available to be used for static IMRT (no VMAT). The couch position is fixed in the bore in AP and LR directions. High density materials, such as the cryostat pipe and treatment couch, reduce the available irradiation angles. The 1.5 T magnetic field, has an impact on the dose deposition, e.g. due to the electron return effect (ERE) at regions of large density changes (i.e., tissue to air) [5] and the shifting of the build-up region

toward the skin [6]. For rectal cancer with a PTV located close to the skin in the dorsal side of the patient, this can result in unacceptable high doses in the patient's back, which has to be controlled in (automated) treatment planning [7].

Automated planning is a hot topic in current radiotherapy research [8–11]. A recently published review by Hussein et al. [12] has highlighted possibilities for enhanced plan quality compared to manual planning, accompanied with clear reductions in hands-on planning time.

At the Erasmus MC, Erasmus-iCycle has been developed for fully automated multi-criterial planning. For each patient a single Pareto-optimal plan is generated. Treatment site specific configurations ('wish-lists'), containing hard constraints and prioritized objectives, are used to ensure that Erasmus-iCycle generated plans are also clinically favorable [8,9,12]. In the plan generation for a patient, the objective functions are sequentially minimized in order of assigned priority while avoiding violations of imposed constraints. Wish-lists are

created in iterative tuning procedures that ensure automatic generation of treatment plans maximally complying with the clinical planning aims, including their tradeoffs [12,13]. Initially, the goal of a wish-list creation is mimicking the MANplan quality. Subsequently, the process has an intrinsic drive to beat the MANplan quality [12,13]. Many studies have demonstrated superiority of Erasmus-iCycle AUTOplans over MANplans generated with conventional trial-and-error planning [9,14–19]. For clinical application at Erasmus MC, the system is used as a pre-optimizer for automated plan generation in the FDA-approved clinical TPS [9,14–19].

In this study, we developed a workflow for fully automated multi-criterial planning for IMRT at the Unity MRL. AUTOplans for rectal cancer patients were compared with MANplans regarding planning workload and time, plan quality, treatment time and delivered MU. Moreover they were checked for dosimetric delivery accuracy.

Material and methods

Patients

Planning CT-scans of 23 rectal cancer patients, previously treated at the NKI (The Netherlands Cancer Institute, Amsterdam), were included in this study. The delineated CTV consisted of the GTV, expanded isotropically with a margin of 10 mm for subclinical disease, plus regional lymph nodes (mesorectal, iliac, and depending on GTV location and N-stage, obturator and/or presacral) with a 5 mm margin. To construct the PTV, the CTV was anisotropically expanded with a margin of 10 mm in all directions except for an expansion up to 15 mm anterior from the mesorectal region [3]. The average PTV volume was 1126 cc, range [781–1530 cc]. A single composite organ at risk (OAR) was constructed as defined in the clinical protocol, consisting of the bowel bag and the bladder, but excluding the overlap region with the PTV. A back structure, was constructed as a helper structure posterior to the PTV (visible in Figure 3), to avoid unacceptable high dose in the back of the patient, arising from the close proximity of the PTV to the skin, and the ERE (relative electron density of the couch matrass $\sim$0.1) and shifted build-up related to the high magnetic field.

Manplanning

MANplanning was performed with version 5.4 of the clinical Unity Monaco TPS (Elekta AB, Stockholm, Sweden), using the structures described in the previous section. MANplans were made by planners experienced in planning for rectal cancer patients according to the local planning control, without any time constraints . The planners did not have prior knowledge of the AUTOplans.

For all patients a Step-and-Shoot IMRT plan was generated for a fixed beam arrangement, consisting of nine beams at gantry angles 0°, 30°, 60°, 90°, 160°, 200°, 270°, 300° and 330° all avoiding irradiation through the cryostat pipe and high attenuation regions of the MRL treatment couch. Because of the specific MRL couch/bore geometry

(Introduction), the MRL isocenter and the center of mass of the PTV did not generally coincide; the isocenter was fixed relative to the couch in LR- and AP directions, i.e., independent of the position of the patient's PTV, while in cranial-caudal direction it was set in the center of the PTV beam eye view.

Prescribed dose for all treatment plans was 50 Gy delivered in 25 fractions. For clinical acceptability, the PTV coverage ($V_{95\%}$) had to exceed 99% with $V_{107\%}<1\%$. Moreover, the maximum dose in the back-structure should not exceed 40 Gy. Additional planning aims were 1) a low OAR D_{mean}, 2) a low patient V_{40Gy}, and 3) a PTV D_{mean} close to the prescribed dose. Clinically used dose calculation and segment settings were applied (i.e., 3 mm dose calculation grid spacing, 1% Monte Carlo dose uncertainty, 2 mm beamlet width. Minimum segment area and width of 16 cm^2 and 5 mm, respectively).

Autoplanning

A fully automated two-step workflow was developed for generation of MRL AUTOplans. In the first step, Erasmus-iCycle was used for multi-criterial fluence map optimization (FMO). To this purpose, the dose calculation engine as used in the MRL TPS [20,21] was also coupled to Erasmus-iCycle for high accuracy dose calculations in the 1.5 T magnetic field. In the next step, the MRL TPS was used to convert the FMO plan into a deliverable IMRT plan [13].

Five of the 23 included patients were used for wish-list generation, based on the same planning goals and with the same treatment aim as used for MANplanning (Manplanning section of Materials and methods). The final wish-list, as presented in Table 1, was created in collaboration with the treating clinician (BvT) for automated treatment plan generation with clinically desired tradeoffs between all planning aims.

A series of maximum dose constraints for concentric shells around the PTV was used to steer the dose conformality (i.e., controlling unacceptable spread out of dose). A maximum dose constraint on the 1 cm entrance dose shell (excluding the back structure posterior to the PTV) was used to control the skin dose. A separate maximum dose constraint was assigned to the back structure in order to steer on the potentially enhanced dose in the back of the patient related to anatomy and the high magnetic field (Patients section of Materials and methods). A generalized Equivalent Uniform Dose (gEUD) constraint with emphasis on the high-dose ($k=20$) was used to control the hot spots in the target. The requested PTV coverage was obtained using a Logarithmic Tumor Control Probability (LTCP) function [22] as the highest priority objective. Second priority was assigned to the mean dose in the composite OAR, to be reduced to the full extent, i.e., to the minimum possible value. The dose pushed away from the OAR was further optimized with the PTV shell objectives with priorities 3 and 4. The fifth priority objective was added to deal with the clinical aim that the PTV mean dose should approximate the prescribed dose. The aim of the 6th priority objective was to further reduce dose in the

Table 1. Wish-list for automated rectal cancer treatment planning for an MRL.

Constraints			
	Structure	*Constraint function*	*Limit*
	PTV	gEUD(20)	$< 103\%$ of PD
	Back*	Maximum dose	$< 38\,$Gy
	PTV shell at 5 mm	Maximum dose	$< 95\%$ of PD
	PTV shell at 1 cm	Maximum dose	$< 90\%$ of PD
	PTV shell at 3 cm	Maximum dose	$< 70\%$ of PD
	PTV shell at 5 cm	Maximum dose	$< 65\%$ of PD
	PTV shell at 7 cm	Maximum dose	$< 50\%$ of PD
	1 cm entrance dose shell*	Maximum dose	$< 50\%$ of PD
Objectives			
Priority	*Structure*	*Aim & objective function*	*Goal value (Sufficient)*
1	PTV	↓ LTCP(95% of PD,α=0.8)	0.06 (0.06)
2	OAR	↓ Mean dose	0
3	PTV shell at 7cm	↓ Maximum dose	0
4	PTV shell at 2cm	↓ Maximum dose	60% of PD
5	PTV	↑ Mean dose	PD (PD)
6	OAR	↓ gEUD(10)	0

PD: Prescribed Dose (50 Gy); gEUD(k): generalized Equivalent Uniform Dose; k: volume parameter, LTCP(PD,α): Logarithmic Tumor Control Probability [22], with α : cell sensitivity; OAR: composite organ at risk; ↓: minimization; ↑: maximization.
*Posterior to the PTV, the entrance dose shell was replaced by the back structure for separate steering on high dose in the back.

OAR (see also priority 2) with an emphasis on high doses (gEUD with $k = 10$). The same segmentation, MRL specific settings and beam angles as in MANplanning were applied in AUTOplanning.

Plan comparisons

For consistent dosimetric comparisons of AUTOplans with MANplans based on equal PTV coverage, all plans were first rescaled such that exactly 99% of the PTV received 95% of the prescribed dose (as clinically requested), implying that in all plans the near minimum dose, $D_{99\%}$, was equal to 95% of the prescribed dose. In line with the clinical planning aims (Manplanning section 2 of Materials and methods), we then compared PTV $V_{107\%}$, PTV D_{mean}, OAR D_{mean} and patient V_{40Gy}.

The conformality index (CI, $V_{95\%}/V_{PTV}$) and homogeneity index (HI, $100*(D_{1\%,PTV} - D_{99\%,PTV})/D_{50\%,PTV}$) were also evaluated, as well as planning times, numbers of MU, and treatment delivery times. Two-sided paired Wilcoxon signed rank tests were used for statistical analyses using a $p < .05$ as significance level.

Dosimetric plan QA

For a subset of 5 arbitrarily selected patients, dosimetric QA was performed at the MRL for the AUTOplan using the Octavius 4D phantom and array (PTW, Freiburg, Germany). Gamma evaluations were performed for the high dose region ($>50\%$) with 3% dose difference relative to the maximum dose and 3 mm distance to agreement [3%/3 mm] criteria, as applied in clinical practice at NKI.

Results

All generated MANplans and AUTOplans satisfied the requirements for clinical acceptability (Manplanning section 2 of Materials and methods).

Table 2. Comparison of dosimetric plan parameters for MANplans and AUTOplans.

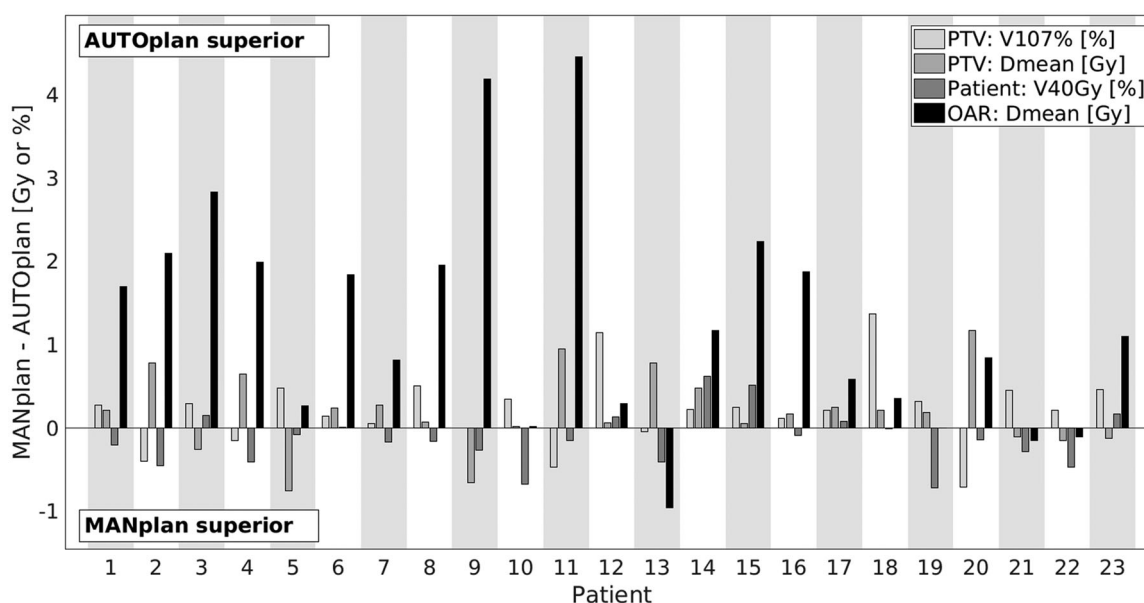|	MANplans		MANplans − AUTOplans		
	Mean	SE	Mean	Range	*p*-Value
PTV					
$V_{95\%}$ [%]	99*	–	0*	–	–
$V_{107\%}$ [%]	0.4	0.1	0.2	[−0.7 − 1.4]	<.01
D_{mean} [%]	50.2	0.3	−0.2	[−1.2 − 0.8]	.04
CI [−]	1.1	0.0	−0.1	[−0.1 − 0.0]	<.01
HI [%]	9.7	0.1	0.8	[−1.0 − 2.5]	.02
OAR					
D_{mean} [Gy]	18.9	0.5	1.3	[−1.0 − 4.5]	<.01
Patient					
V_{40Gy} [%]	10.9	0.7	−0.1	[−0.7 − 0.6]	.04

SE: standard error; PTV: planning target volume; OAR: organ at risk; CI: conformity index; HI: homogeneity index.
*All plans normalized to 99%.

Table 2 shows population mean MANplan dosimetric parameters and mean differences with AUTOplans. With equal PTV coverage, AUTOplans had on average a small advantage in PTV $V_{107\%}$, PTV D_{mean}, and homogeneity index (HI). More important, the OAR D_{mean} was reduced by on average 1.3 Gy (6.9%, $p < .001$)), with a maximum of 4.5 Gy (23.8%). The AUTOplans had slightly increased patient V_{40Gy} (0.1%) and CI (0.1).

Figure 1 displays absolute dosimetric differences between MANplans and AUTOplans for each patient. Positive differences (except for PTV D_{mean}) are in favor of the AUTOplans. For 20 of the 23 study patients (87%), the automated workflow resulted in a lower mean dose in the OAR. PTV $V_{107\%}$ and PTV D_{mean} were improved for 18/23 (78%) and 17/23 (74%) of the patients respectively. For 16/23 patients (70%) the patient V_{40Gy} was enhanced in the AUTOplans. Figure 2 shows the MANplan and the AUTOplan dose distribution for an example patient.

Figure 3 shows for an example patient how the automated workflow defined by the wish-list (Table 1) could avoid unacceptable high dose in the back of the patient caused by the ERE and shifted build-up resulting from the 1.5 T magnetic field.

Figure 1. Absolute differences in dosimetric plan parameters between the MANplans and AUTOplans for all 23 patients. Positive values indicate a better AUTOplan. The first 5 patients were used to train the automated treatment planning workflow.
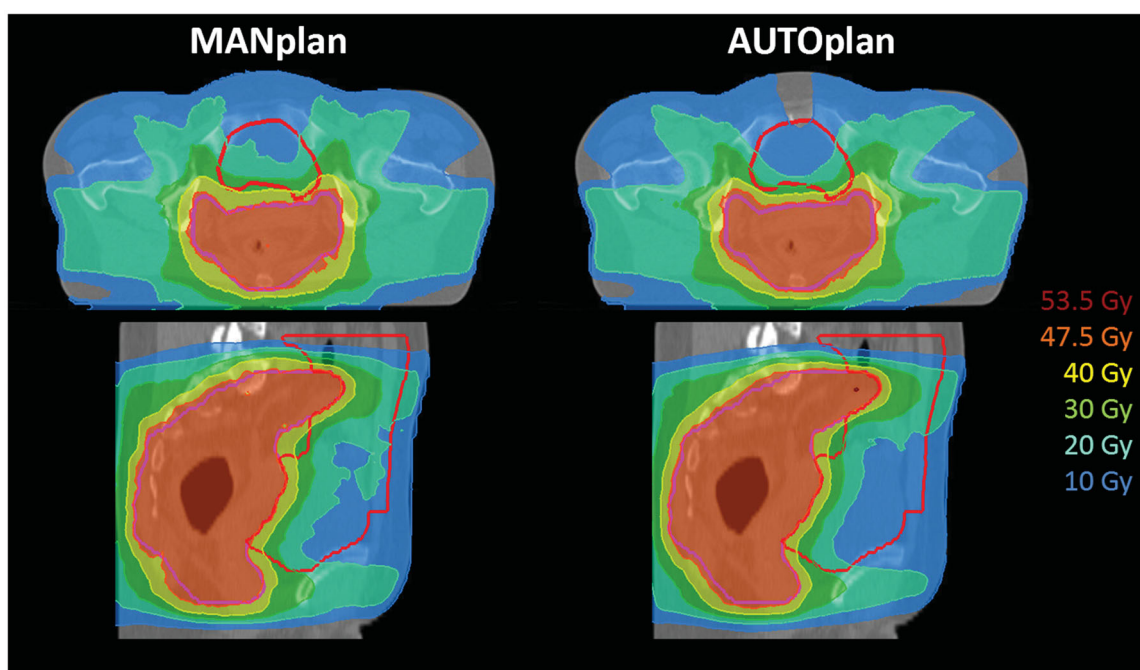
Figure 2. Dose distributions for the MANplan (left) and AUTOplan (right) for patient 14 (See Figure 1). The AUTOplan had clearly reduced dose in the OAR. Top: axial view, bottom sagittal view. Magenta contour = PTV, Red contour = OAR.

### Planning times, Monitor Units and delivery times

Planning times reduced from ∼4–6 h per patient for MANplans (mainly hands-on time) to ∼1 h per patient for AUTOplans (mainly computational time). The number of monitor units (MU) reduced from 677 ± 214 for MANplans to 589 ± 90 for AUTOplans ($p < .01$) MANplans had estimated delivery times of 321 ± 65 s which reduced to 274 ± 47 s for the AUTOplans ($p < .01$).

Dosimetric plan QA

The QA measurements showed a 100% gamma passing rate for all 5 patients. The median gamma ranged from 0.19 to 0.33, compared to 0.34 in the clinic.

Discussion

In this study we have developed the first system for fully automated multi-criterial planning for a high magnetic field MR-Linac (MRL). To this purpose, a Monte Carlo dose calculation engine, suited for high accuracy dose calculations in a 1.5 T magnetic field, was coupled to our in-house Erasmus-iCycle optimizer. An automated workflow including Erasmus-iCycle and the clinical MRL TPS was configured for rectal cancer treatment with an MRL at the NKI. AUTOplans were superior to MANplans, especially regarding sparing of bladder and bowel bag, in line with the observed benefits of automated planning for regular linacs [9,15,18,19,23].
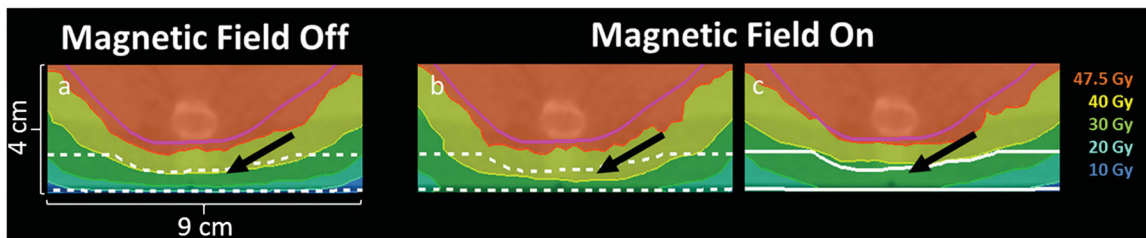
Figure 3. Parts of axial dose distribution for patient 14 (in PTV and posterior to PTV) (a) clinically acceptable dose distribution without magnetic field (6 MV conventional linac plan). (b) clinically unacceptable dose distribution with magnetic field (MRL plan) but no dose control by back structure; too high dose in back structure (arrow) related to ERE and enhanced build-up due to the magnetic field. (c) clinically acceptable dose distribution with magnetic field (MRL plan) and dose control using the back structure. Pink contour = PTV, dashed white contour = inactive back structure, solid white contour = active back structure. The treatment couch matrass is located right below the back structure.

Moreover, AUTOplanning allowed reductions of 13% in the number of delivered MU and 15% in the treatment time. The planning time reduced from 4–6 h per patient to around 1 h, the latter mainly consisting of computer calculation time. It was shown that automated treatment planning was feasible for MRL rectum cancer treatment, despite the presence of a 1.5 T magnetic field that influences the dose deposition (i.e., electron return effect and shallower build-up dose). Also, the limitations in the isocenter placement, collimator rotation and beam angles, were no limiting factors in the automated treatment planning workflow.

In this paper, the analyzed composite OAR consisted of the bowel bag and the bladder, excluding the overlap with the PTV. An additional analysis (not presented) for an OAR that included the overlap region resulted in similar conclusions regarding plan quality differences. This could be expected as for all plans in this study (clinically and automatically generated) the overlap region was treated as PTV, so a homogenous coverage with high dose was always requested with high priority.

In this study, all plans were generated with the same beam configuration. Moreover, the applied number of beams was relatively high [9]. Therefore, we believe that plan robustness issues due to the presence of the high-magnetic field and daily variations in anatomy may be small, and similar for clinically and automatically generated plans. Prior to clinical application this can be verified for a group of patients.

At the NKI, rectal cancer patients are currently treated using a library-of-plans (LoP) strategy [15,24,25], requiring patient-specific plan libraries with plans for various patient anatomies. Automated plan generation can then greatly reduce the planning workload, as was also observed for cervical cancer treatment [26]. In addition, the use of the same wish-list for all library plans could guarantee similar tradeoffs between treatment goals along the entire treatment of the patient, which is hard to achieve with manual treatment planning. The superior image quality of in-room MR compared to cone beam CT might render use of libraries with enhanced numbers of plans possible. Creating these extended libraries would practically only be feasible with automatic plan generation.

Tools for on-line adaptive strategies are currently applicable in the clinical TPS, including the use of LoPs. Compared to current clinical practice, the automated LoP-plan generation could increase plan quality of the adaptive LoP workflow. However, full re-planning based on the anatomy of the day can potentially further enhance plan quality. For the longer future, multi-criterial optimizers are being developed that are fast enough for daily on-line re-planning based on acquired MR images [27,28], which would require the use of synthetic CT generation for online dose calculations. The daily MR-based re-planning can then replace in principle the plan library approach, ensuring maximum daily plan quality while considering also the dose delivered in previous fractions. Clinical application of daily MR-based re-planning would require a sufficiently fast and safe procedure for the daily contouring, preferentially not dependent on a clinician that needs to stay at the treatment unit.

In this study, all AUTOplans were generated for a fixed beam angle class solution, as used at the NKI. However, Erasmus-iCycle also features individualized beam angle selection. In a future study we will use this option to investigate potential advantages of optimized, patient-specific beam arrangements. With the developed automated planning workflow, many alternative plans with various beam arrangements can be easily generated without user interaction. Combined with the use of a single wish-list for all beam angle configurations, a lot of intrinsic bias in conventional trail-and-error treatment planning studies can be avoided [29]. The investigated MRL system only allows coplanar treatment. In previous studies using automated planning we observed superiority of non-coplanar treatment compared to coplanar [23]. However, in [23] equal PTV margins were used for the coplanar and non-coplanar plans. Due to the advanced imaging, it is to be expected that margins can be largely reduced for the MRL. In future studies we will use automated planning to compare MRL treatment with small margins with non-coplanar treatment at a regular treatment unit with larger margins.

In this paper we studied automated planning for the 1.5 T Unity MR-linac. To the best of our knowledge fully automated planning has not yet been investigated for the MRIdian treatment unit (Viewray Inc, Cleveland OH) with an integrated 0.35 T MR scanner. Bohoudi et al. developed an artificial neural network for knowledge-based prediction of OAR constraints for pancreatic patients, which were used to guide conventional, manual generation of final plans [30]. The Network was trained with plans that were manually generated with the clinical TPS. In a validation study for independent cases (not used for network training), plans

generated with the help of the neural network and corresponding clinical plans had similar quality.

Automated planning is currently not generally available for the Unity MRL. However, the manufacturer is working on a commercial implementation of the system presented here.

Conclusion

A system for fully automated multi-criterial planning for a 1.5 T MR-Linac has been developed and tested for rectal cancer patients. The impact of the high magnetic field on the dose distribution could be controlled. The quality of the automatically generated plans superseded that of plans generated with conventional trial-and-error planning. Moreover, automated planning resulted in reduced MU and treatment time and a major reduction in manual planning workload. Automated planning has a high potential for further improvement of advanced MRL treatment.

Acknowledgments

Disclosure statement

ORCID

Rik Bijman http://orcid.org/0000-0003-1915-3739

References

[1] Raaymakers BW, Lagendijk JJ, Overweg J, et al. Integrating a 1.5 T MRI scanner with a 6 MV accelerator: proof of concept. Phys Med Biol. 2009;54(12):N229–N237.

[2] Raaymakers BW, Jurgenliemk-Schulz IM, Bol GH, et al. First patients treated with a 1.5 T MRI-Linac: clinical proof of concept of a high-precision, high-field MRI guided radiotherapy treatment. Phys Med Biol. 2017;62(23):L41–L50.

[3] Nijkamp J, de Jong R, Sonke JJ, et al. Target volume shape variation during hypo-fractionated preoperative irradiation of rectal cancer patients. Radiother Oncol. 2009;92(2):202–209.

[4] Kerkmeijer LG, Fuller CD, Verkooijen HM, et al. The MRI-linear accelerator consortium: evidence-based clinical introduction of an innovation in radiation oncology connecting researchers, methodology, data collection, quality assurance, and technical development. Front Oncol. 2016;6:215.

[5] Raaijmakers AJ, Raaymakers BW, Lagendijk JJ. Integrating a MRI scanner with a 6 MV radiotherapy accelerator: dose increase at tissue-air interfaces in a lateral magnetic field due to returning electrons. Phys Med Biol. 2005;50(7):1363–1376.

[6] Raaymakers BW, Raaijmakers AJ, Kotte AN, et al. Integrating a MRI scanner with a 6 MV radiotherapy accelerator: dose deposition in a transverse magnetic field. Phys Med Biol. 2004;49(17):4109–4118.

[7] van de Schoot AJAJ, van den Wollenberg W, Carbaat C, et al. Evaluation of plan quality in radiotherapy planning with an MR-Linac. Physics and Imaging in Radiation Oncology. 2019;10:19–24.

[8] Breedveld S, Storchi PR, Voet PW, et al. iCycle: integrated, multi-criterial beam angle, and profile optimization for generation of coplanar and noncoplanar IMRT plans. Med Phys. 2012;39(2):951–963.

[9] Voet PW, Dirkx ML, Breedveld S, et al. Fully automated volumetric modulated arc therapy plan generation for prostate cancer patients. Int J Radiat Oncol Biol Phys. 2014;88(5):1175–1179.

[10] Zhang X, Li X, Quan EM, et al. A methodology for automatic intensity-modulated radiation treatment planning for lung cancer. Phys Med Biol. 2011;56(13):3873–3893.

[11] Purdie TG, Dinniwell RE, Fyles A, et al. Automation and intensity modulated radiation therapy for individualized high-quality tangent breast treatment plans. Int J Radiat Oncol Biol Phys. 2014;90(3):688–695.

[12] Hussein M, Heijmen BJM, Verellen D, et al. Automation in intensity modulated radiotherapy treatment planning-a review of recent innovations. Br J Radiol. 2018;91(1092):20180270.

[13] Heijmen B, Voet P, Fransen D, et al. Fully automated, multi-criterial planning for Volumetric Modulated Arc Therapy - An international multi-center validation for prostate cancer. Radiother Oncol. 2018;128(2):343–348.

[14] Voet PW, Dirkx ML, Breedveld S, et al. Toward fully automated multicriterial plan generation: a prospective clinical study. Int J Radiat Oncol Biol Phys. 2013;85(3):866–872.

[15] Sharfo AW, Voet PW, Breedveld S, et al. Comparison of VMAT and IMRT strategies for cervical cancer patients using automated planning. Radiother Oncol. 2015;114(3):395–401.

[16] Della Gala G, Dirkx MLP, Hoekstra N, et al. Fully automated VMAT treatment planning for advanced-stage NSCLC patients. Strahlenther Onkol. 2017;193(5):402–409.

[17] Buergy D, Sharfo AW, Heijmen BJ, et al. Fully automated treatment planning of spinal metastases – a comparison to manual planning of Volumetric Modulated Arc Therapy for conventionally fractionated irradiation. Radiat Oncol. 2017;12(1):33.

[18] Buschmann M, Sharfo AWM, Penninkhof J, et al. Automated volumetric modulated arc therapy planning for whole pelvic prostate radiotherapy. Strahlenther Onkol. 2018;194(4):333–342.

[19] Sharfo AWM, Stieler F, Kupfer O, et al. Automated VMAT planning for postoperative adjuvant treatment of advanced gastric cancer. Radiat Oncol. 2018;13(1):74.

[20] Hissoiny S, Ozell B, Bouchard H, et al. GPUMCD: a new GPU-oriented Monte Carlo dose calculation platform. Med Phys. 2011;38(2):754–764.

[21] Hissoiny S, Raaijmakers AJ, Ozell B, et al. Fast dose calculation in magnetic fields with GPUMCD. Phys Med Biol. 2011;56(16):5119–5129.

[22] Breedveld S, Storchi PR, Keijzer M, et al. A novel approach to multi-criteria inverse planning for IMRT. Phys Med Biol. 2007;52(20):6339–6353.

[23] Rossi L, Sharfo AW, Aluwini S, et al. First fully automated planning solution for robotic radiosurgery – comparison with automatically planned volumetric arc therapy for prostate cancer. Acta Oncol. 2018;57(11):1490–1498.

[24] Heijkoop ST, Langerak TR, Quint S, et al. Clinical implementation of an online adaptive plan-of-the-day protocol for nonrigid motion management in locally advanced cervical cancer IMRT. Int J Radiat Oncol Biol Phys. 2014;90(3):673–679.

[25] Beekman C, van Triest B, van Beek S, et al. Margin and PTV volume reduction using a population based library of plans strategy for rectal cancer radiotherapy. Med Phys. 2018;45(10):4345–4354.

[26] Sharfo AW, Breedveld S, Voet PW, et al. Validation of Fully Automated VMAT Plan Generation for Library-Based Plan-of-the-Day Cervical Cancer Radiotherapy. PLoS One. 2016;11(12):e0169202.

[27] van Haveren R, Heijmen BJM, Breedveld S. Automatically configuring the reference point method for automated multi-objective treatment planning. Phys Med Biol. 2019;64(3):035002.

[28] van Haveren R, Ogryczak W, Verduijn GM, et al. Fast and fuzzy multi-objective radiotherapy treatment plan generation for head and neck cancer patients with the lexicographic reference point method (LRPM). Phys Med Biol. 2017;62(11):4318–4332.

[29] Rossi L, Breedveld S, Heijmen BJ, et al. On the beam direction search space in computerized non-coplanar beam angle optimization for IMRT-prostate SBRT. Phys Med Biol. 2012;57(17): 5441–5458.

[30] Bohoudi O, Bruynzeel AME, Senan S, et al. Fast and robust online adaptive planning in stereotactic MR-guided adaptive radiation therapy (SMART) for pancreatic cancer. Radiother Oncol. 2017; 125(3):439–444.